Prediction of Rope Bending Fatigue Life Based on Wire Breaking Rate

P. Freddi
Mechanical Engineer
University of Brescia
Department of Mechanical and Industrial Engineering
Italy

L. Solazzi
Associate Professor
University of Brescia
Department of Mechanical and Industrial Engineering
Italy

G. Donzella
Full Professor
University of Brescia
Department of Mechanical and Industrial Engineering
Italy

Steel wire ropes offer manufacturer-independent safety performance, while the durability performance can be different. To assess the damage status of a wire rope during its service, fail-safe methods are used, so it is necessary to know the progression of the damage to apply them. This paper proposes an analytical method for estimating the fatigue life of steel wire ropes. Using a dimensionless analysis, the characteristic damage curve of each rope category has been suggested, setting the basis of a predictive maintenance procedure extendable to all areas of rope application where bending fatigue is the first discard criterion for rope replacement. Rotary bending fatigue tests are performed on different rope construction specimens, and the evolution of broken wires is monitored. It has been demonstrated that the trend of breakage level is exponential with time, regardless of the type of rope and the stress level imposed.

Keywords: *Steel wire rope; fatigue life prediction; bending fatigue; broken wire; predictive maintenance.*

1. INTRODUCTION

The study of the mechanical fatigue behavior of steel wire ropes involves the solution of different kinds of problems regarding geometry (diameters, lay lengths, curvatures, etc.), elasticity (stresses in the wires due to tension and bending over pulleys or winches, primary and secondary bending, torsion, local contacts) [1-5], plasticity (plastic deformations due to local crushing, tensile or bending failure, etc.); metallurgy and technology (steel composition and microstructure, heat and mechanical treatments, metallographic structure, static and fatigue resistance characteristics of the wire, quality, and characteristics of the wire rope core, characteristics, and effect of the lubricant, etc.), and finally the study of wire rope resistance in each application (industrial lifting, mining, tenso-structures, off-shore, etc.) [6-8].

To determine the extent of these effects, a series of theories have been developed over the years, from the early 50's until today, to find a correct method of calculation [9-11]. The approaches for studying wire ropes can be divided into two groups. The first approach is based on continuous mechanics and, more recently, based on finite element numerical simulations [12,13]. The application of this approach is particularly complex, depending on many factors and how they vary; therefore, the investigations are limited to the study of individual wires [14-18]. Moreover, since the rope is composed of several wires laid to form strands that are placed to form the rope, the numerical problem is strongly non-linear, making the computational cost practically impossible for the available resources. To overcome this obstacle, in the literature, there are simplified models to perform a first estimation of the stresses to which the rope is subject.

The second approach is based on empirical methods by carrying out experimental tests representative of real application cases [19-21]. New approaches use derived parameters to determine fatigue behavior, such as methods based on energy considerations [22,23]. Some methods assume the rope temperature variation during service as an indicator of the stress level, then extrapolate it as an index of fatigue resistance of the rope [24,25], following a more general approach pro–posed for fatigue prediction in steels [26,27].

These methods need several laboratory tests to generalize the results for industrial environments.

In order to simplify the rope design and its use, we still refer only to the rope's breaking load because it is a parameter easy to evaluate through a tensile test. Nowadays, the end user is demanding and requires guarantees on the rope performance during its service. The rope variables, the installation on which it is mounted, the environmental conditions, and the operator should therefore be considered in calculating fatigue life [28,29]. In addition, it should also be possible to determine the rope life in a not-debatable way. Standards are used to determine when a rope should be discarded (in the hoisting field, the most commonly used standard is ISO 4309:2017) that propose criteria for evaluating the rope damage during its service.

Another question is how often a rope should be inspected: it will depend on the damage evolution speed, so many researches were concentrated on predic–ting the rope's life [25, 30-32].

This work is part of this line of research, whose main purpose is to evaluate the fatigue behavior of the rope in relation to the progression of the number of bro–ken wires in the rope [33-36], the main indicator used for the rejection of a rope under fatigue loading. Specifically, this experimental work studies four diffe–rent rope constructions, subjecting them to rotating bending fatigue by varying the load condition by setting

Received: November 2022, Accepted: January 2023
Correspondence to: Prof. Luigi Solazzi, University of Brescia (IT), Department of Mechanical and industrial Engineering, Via Branze 38, I-25123 Brescia, Italy
E-mail: luigi.solazzi@unibs.it
doi: 10.5937/fme2301059F

the D/d ratio and monitoring the progression of broken wires in order to evaluate an empirical model to predict the wire rope fatigue life.

2. EXPERIMENTAL DETAILS

Rotating bending fatigue tests were carried out on rope specimens shown in par. 2.1 throughout the testing apparatus described in par. 2.2, which allows for varying the D/d ratio and the specimen rotation speed.

Each test was carried out at a fixed D/d ratio and constant rotation speed. During each test, the following data were detected: the specimen temperature by means of an infrared thermometer pointed in the center of the specimen, the number of cycles $\bar{N}$ at which the wires break, and the position of the failed wires in the speci–men.

Some preliminary tests were carried out, as des–cribed in par. 2.3, in order to check the result's repeatability.

2.1 Samples description

The specimens were obtained from new ropes, whose detailed specifications are given in Table 1, while in Fig.1, their respective cross-section is shown.

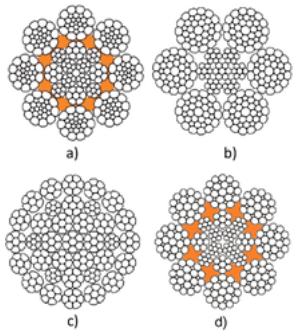

Figure 1. Rope construction of the tested ropes:

a) 8×K26WS-EPIWRC, b) 6×K31WS-IWRC, c) 35x7/35xK7 and d) 8×25F-EPIWRC

Table 1. Specifications of the tested rope samples (K=compacted rope, RH=right hand rope, LH=left hand tope, OL=ordinary-lay rope, LL=lang-lay rope).

Rope construction	Nominal diameter [mm]	Lay length [mm]	Minimum Breaking Force [kN]	Rope grade
8×K26WS-EPIWRC LHOL	22	138	425	1960
6×K31WS-IWRC RHOL	22	139	440	2160
35×7 RHLL	24	159	460	2160
35×K7 RHLL	24	173	572	2160
8×25F-EPIWRC RHOL	22	140	397	1960
8×25F-EPIWRC RHOL	24	161	472	1960

The specimens belong to the six and eight strands, rotation resistant ropes typology, which covers almost 90% of the modern market applications. The cores are IWRC (Independent Wire Rope Core), and two are plastic-coated. All the samples are zinc coated and lubricated with typical grease for off-shore systems. The rope grade (the level of required breaking force) is the most widely used for lifting applications.

2.2 Testing apparatus

The experiments were carried out on a self-made ben–ding fatigue test machine. It is based on a center lathe, in which a neutral spindle with the axle parallel to the motor spindle axle was added to simulate the rope ben–ding on a pulley (similar apparatus in [25,37]). For this reason, the distance between the two spindles' axes is called D, as it is usually called the diameter of the pulley the rope turns around, while the nominal dia–meter of the rope is called d so that the D/d ratio indicates the rope's bending level (Fig.2).

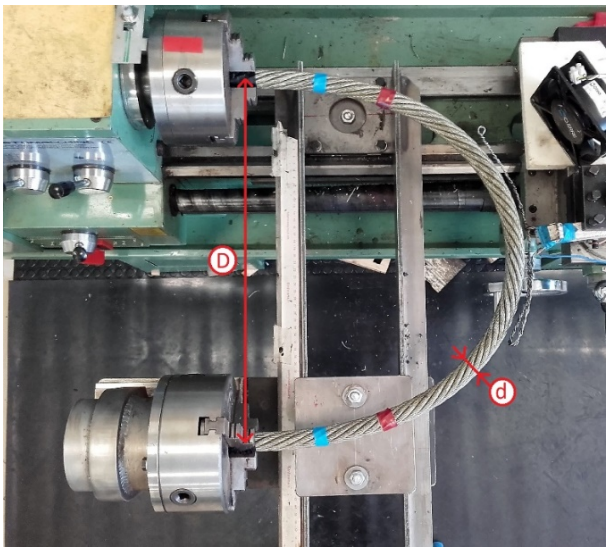

Figure 2. Experimental apparatus used for testing ropes

For these experiments, D/d ratios of 12, 16, and 20 were chosen: D/d=20 is the most common minimum ratio used in lifting, D/d=12 is the minimum ratio that can be set on the test machine, while D/d=16 is inter–mediate between the first two. The two ends of the rope sample are inserted inside the spindles. The impressed curvature and the rotation of the spindles impose a rotating-bending load on the specimen. Therefore, this configuration of the test machine simulates only the bending action in the rope, excluding other types of actions, particularly the tensile load and the interaction with the pulley. The test variables are thus reduced to a minimum number. This allows us to carry out faster tests than classic fatigue tests [34,35,38-40], despite the absence of a pre-tension system. The testing machine is equipped with an automatic wire break detection system. When a wire breaks, it protrudes from the sample profile, hitting an aluminum wire close to the specimen center (Fig.2) and interrupting the lathe motor's power supply to stop the test. In order to take into account the lay orientation of the strands in the rope, the rotation direction of the motor spindle is arbitrarily set clockwise for the left-hand rope and counter-clockwise for the right-hand rope so as to prevent the rope from opening.

To set a common reference rotation speed for the tests, and in order to reduce their duration, it was decided to carry out the tests at the maximum speed permitted by the test device, i.e. 380 RPM, except for the tests reported in par.3.4 which was carried out at 220 RPM due to the power limitation of the testing apparatus.

2.3 Preliminary analysis

Some preliminary tests were carried out to check the result's repeatability and the effect of spindle rotation speed and D/d ratio (which is directly proportional to the stress induced in the specimen [25]), thus allowing to define of the optimum range of these parameters to be used in the subsequent tests.

In each test, the rope damage evolution was monitored by plotting the number of visible broken wires as a function of the number of bending fatigue cycles. The temperature evolution as a function of bending cycles was also recorded in parallel, with a sampling interval of the temperature equal to two minutes.

Fig. 3 shows the results of two 8×K26WS-EPIWRC rope tests with a D/d ratio set at 12 and test speed set at 380 RPM (green and blue line) in order to study the result's repeatability. For each number of broken wires, the average value of the corresponding number of cycles was calculated, resulting in an average curve (red and dashed dot line): it can be seen that the test curves lie within a ± 5% deviation of the average value.

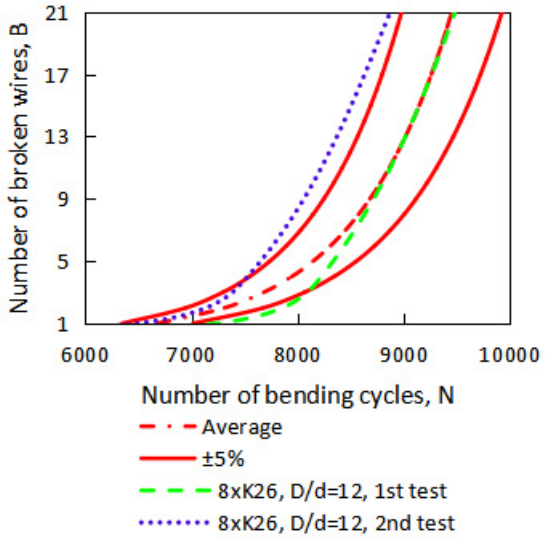

Figure 3. Rope damage evolution for K26WS-EPIWRC rope tests with D/d ratio set at 12 and test speed set at 380 RPM

This variability can be associated with errors due to the slight irregularity of the rope along its length, the variation of temperature and ventilation, the positioning of the rope in the spindles, and measurement inaccuracies. Other tests have shown how wire ropes are particularly stable from this point of view.

The preliminary tests also observed that the relationship between the number of broken wires and the number of bending fatigue cycles could be well approximated by exponential functions.

The temperature variation (with respect to the room temperature) during the fatigue tests presents a typical behavior as reported in Fig.4: it shows an almost linear increase of temperature with cycle number in the initial phase of the test, ascribable to the energy dissipated by friction in the contact zones between the internal wires, depending on the contact pressure and the corresponding frictional forces generated by their relative movement [25]; this initial phase is followed by a plateau where the temperature tends to stabilize, being reached an equilibrium between the heat produced by friction and that exchanged with the environment.

The research in [25] showed that if the maximum temperature reached by the rope during the test remains below 140° C, the test results are not influenced by the temperature value. The temperature was measured during each test to verify this condition. A fan was then used to cool the specimen, allowing higher rotational speed tests without exceeding this threshold.

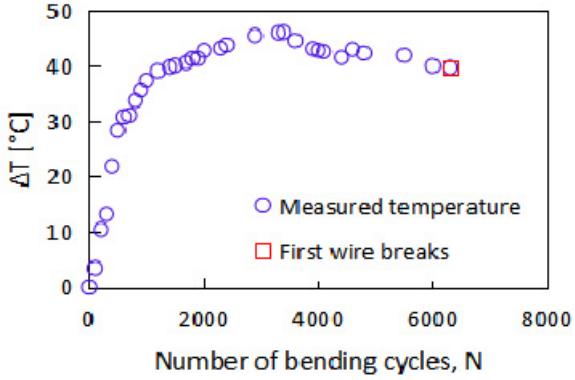

Figure 4. The trend of rope temperature during a rotary bending fatigue test

2.4 Criteria for damage limits

According to the International Standard Organization (ISO 4309:2017), the rope working on a crane must be discarded when the number of visible wire breaks (called "discarding limit" - $\overline{B}_{disc}$) is found in a length range of 6d (i.e., in a rope length equal to 6 times the rope diameter) or 30d (i.e., 30 times of the rope diameter). These numbers depend on the rope construction and the group of mechanisms (M1 to M8).

In our tests, the wires always broke in a segment of rope specimen shorter than 6d length. The tests were, however, not stopped when the discarding limit was reached but were continued beyond this, up to a second limit, called the "stopping limit" ($\overline{B}_{stop}$), with the purpose of investigating the evolution of the bending fatigue damage. The stopping limit was arbitrarily set based on experience and, depending on the specimen typology, as proportional to the number of outer wires of the rope (thus giving more importance to the outer wires, which are the ones subjected to the higher loads): for stranded ropes, $\overline{B}_{stop}$ corresponds to a quarter of the total external wires of the outer strands, while for rotation resistant ropes $\overline{B}_{stop}$ is three times the number of the corresponding discarding limit. For example, the strands of the 8×K26WS-EPIWRC rope have 10 outer wires, for a total of 80 external wires divided by 4 giving $\overline{B}_{stop} = 20$. The numbers of broken wires according to these two criteria are shown in Table 2 for each tested rope.

Table 2. A number of broken wires define each tested rope's discarding limit ($\bar{B}_{disc}$) and stopping limit ($\bar{B}_{stop}$).

Rope construction	$\bar{B}_{disc}$	$\bar{B}_{stop}$
8×K26WS-EPIWRC	9	20
6×K31WS-IWRC	8	18
35×K7	3	9
8×25F-EPIWRC	6	24

The number of bending cycles in which the $\bar{B}_{disc}$ number of wire breaks is reached is called $\bar{N}_{disc}$; similarly, $\bar{N}_{stop}$ is the number of bending cycles in which the $\bar{B}_{stop}$ number of wire breaks is reached.

For each type of rope, three tests were carried out with the D/d ratio set to 12, 16, and 20; the test speed was set at 380 RPM.

3. RESULTS

The following graphs report the number of broken wires as a function of cycle numbers: the markers represent the cumulated number of broken wires detected at each test stop. For all performed tests, wire breaks occurred randomly on the rope samples, both at the crown and valley of the strands.

3.1 8×K26WS-EPIWRC

Fig. 5 shows the test results carried out with the D/d ratio set to 12, 16, and 20. The test at D/d=12 corres–ponds to the highest bending level, with the appro–ximating exponential function: as a consequence of the high stresses, the wires of the outer layer started brea–king after a few thousand loading cycles, in groups of two or more, mainly localized in the valleys between the strands. Due to the cooling system, the specimen temperature remained under 95°C.

The test result with the D/d ratio set to 16 is shown in the same figure. Due to the lower load, the wires started breaking later (after 15000 cycles) and mostly individually: the broken wires were anyway all located again in the valley position. The specimen temperature reached a maximum of 60°C.

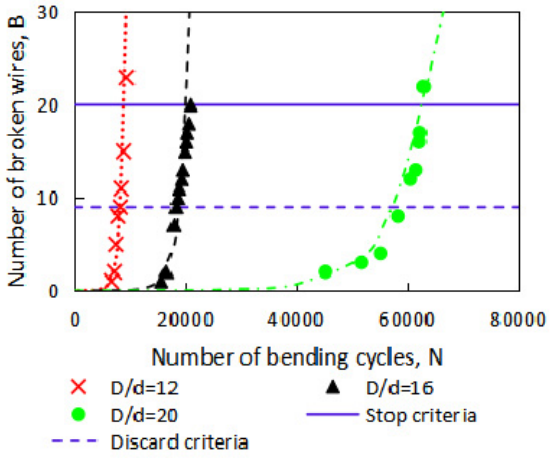

Figure 5. Tests performed on 8×K26WS-EPIWRC rope at D/d=12 (x - redline), D/d=16 (▲- black line), D/d=20(●- green line)

Fig. 5 also shows the test results with the D/d ratio set to 20: in this case, the wires started breaking after 45000 cycles, showing three breaks on the crown of the strands, while the remaining were valley breaks. The maximum test temperature was 55°C.

The main values of the three tests are shown in Table 3.

Table 3. The number of cycles when the discard criteria and stop criteria are reached for 8×K26WS-EPIWRC rope tests

D/d ratio	$\bar{N}_{disc}$	$\bar{N}_{stop}$
12	8300	9400
16	18310	20920
20	58200	62870

3.2 6×K31WS-IWRC

The test results carried out with the D/d ratio set to 12, 16, and 20 are shown in Fig.6.

For the test set to D/d=12, all the broken wires were located in the valleys of the strands. The specimen rea–ched a temperature of 112°C, a higher value than the 8×K26WS-EPIWRC test rope in the same condition, due to the decrease of the contact areas between the wires and a corresponding increase of the contact pressure.

The test result carried out with the D/d ratio set to 16 is reported in the same figure: five wires broke on the crown, and the remaining in the valley. As can be seen, during the initial stage of the test, the broken wires appear individually, then in groupings of two or three. The specimen temperature reached a maximum of 94°C.

Regarding the D/d ratio test set to 20 (Fig.6), the exponential trend is particularly accurate (R^2 is high). Four wires broke on the crown and the remaining in the valley; the max temperature reached during the test was 79 °C.

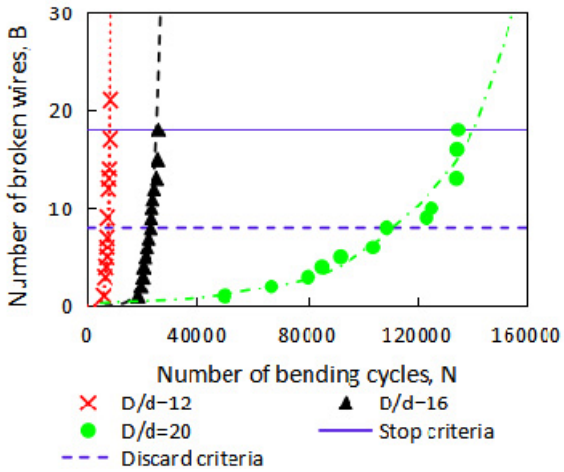

Figure 6. Tests performed on 6×K31WS-IWRC rope at D/d=12 (x - redline), D/d=16 (▲- black line), D/d=20 (●- green line)

The main values of the three tests are shown in Table 4.

Table 4. The number of cycles when the discard criteria and stop criteria are reached for 6×K31WS-IWRC rope tests

D/d ratio	$\bar{N}_{disc}$	$\bar{N}_{stop}$
12	7360	8430
16	23140	26070
20	108950	134800

3.3 35×K7

In the case of rotation-resistant type ropes, there is a possibility that the majority of wires break internally, thus being difficult to detect them by a visual inspection. For this reason, after completion of the tests, it was necessary to open the specimens to establish if any detrimental internal damage happened.

The result of the tests is reported in Fig. 7.

For the test set to D/d=12: the first five broken wires were observed on the crown, while the remaining were on the valley. After removing the external strands at the end of the test, 9 further breaks on the crown of the core were detected: for this test, the internal broken wires were equal to those found on the outer layer. Therefore, it has to be noted that the allowable number of visible broken wires for a rotation-resistant rope is less than that for a single-layer or parallel-closed rope, confirming the prescription given by the standards and shown in Table 2. The maximum temperature was 95°C.

The test result with the D/d ratio set to 16 is shown in Fig.7. In this case, they happened 2 crown breaks and 9 valley breaks; internally, the core presented 9 wire breaks. The maximum temperature was 87°C.

The test with D/d set to 20 is shown in Fig.7. The internal broken wires were 26. The temperature reached a maximum of 63°C.

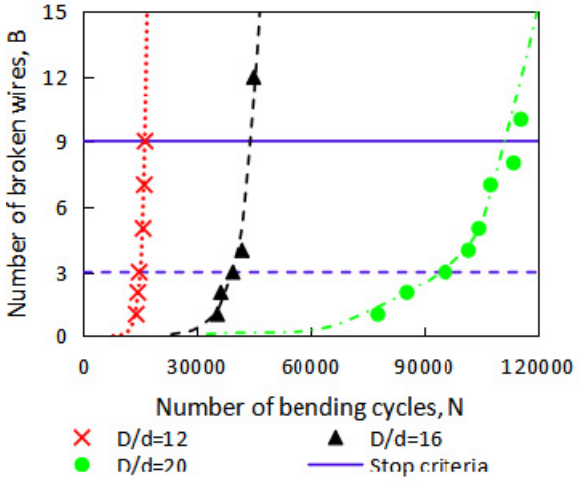

Figure 7. Tests performed on 35×K7 rope at D/d=12 (x - redline), D/d=16 (▲- black line), (●- green line)

The main values of the three tests are shown in Table 5.

Table 5. The number of cycles when the discard criteria and stop criteria are reached for 35×K7 rope tests

D/d ratio	$\bar{N}_{disc}$	$\bar{N}_{stop}$
12	13075	15340
16	39430	44860
20	95480	115410

3.4 Rope diameter effect

Specific tests were carried out to evaluate the effect of a rope diameter variation. Two specimens were obtained from a rope of 8×K25F-EPIWRC construction with diameters of 22 mm and 24 mm and tested with a D/d ratio set to 16. In this case, the test speed rotation was set to 220 RPM (because this was the maximum speed admitted by the testing machine for the 24 mm 8×K25F-EPIWRC diameter sample). By varying the diameter of the rope, the wire size and the construction of the rope change proportionally. The results of the tests are shown in Fig. 8.

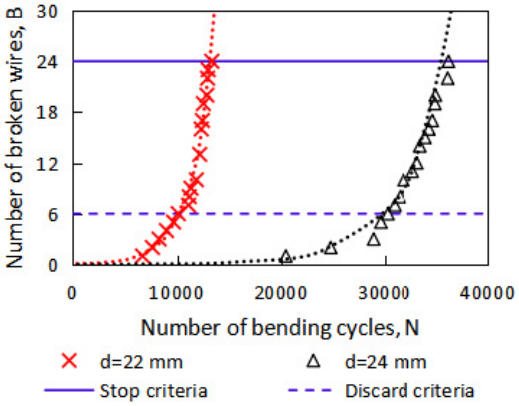

Figure 8. Comparison of the broken wire trend between ropes with the same construction but different diameter

During both tests, some filler wires leaned out the profile of the specimens as a consequence of the high bending load, without, however, affecting the limit of the discard criteria, as filler wires are not included in the values of $\bar{B}$. By increasing the rope sample diameter, the fatigue life of the rope (i.e., the number of cycles) has risen by 3 times referring to the first broken wire and the discard criteria, whereas by 2.7 times referring to the stop criteria.

The main values of the two tests are shown in Table 6.

Table 6. The number of cycles when the discard criteria and stop criteria are reached for 8×K25-EPIWRC rope tests

d	$\bar{N}_{disc}$	$\bar{N}_{stop}$
22	10130	13350
24	30260	36200

3.5 Compaction effect

In order to evaluate the compaction effect on fatigue life, tests on similar ropes were carried out. The first specimen was obtained from a 35×K7 rope, whereas the second was obtained from a 35×7 rope (non-compacted and rotation-resistant), both with a diameter of 24 mm.

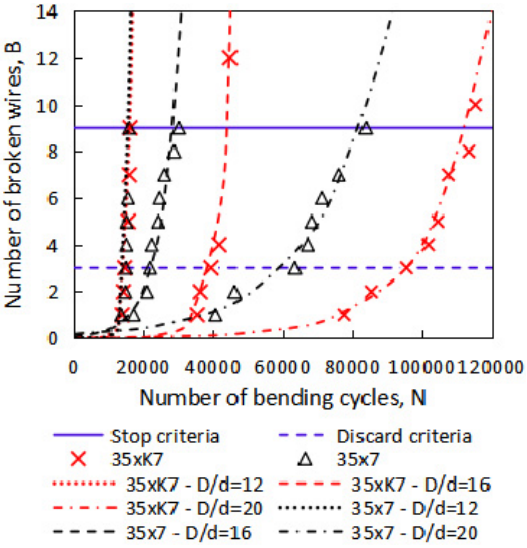

Figure 9. Comparison of the broken wire trend between a compacted and a not compacted rope for different D/d

Three tests for each rope were carried out, setting the D/d ratio to 12, 16, and 20 (Fig.9) at 380 RPM.

The specimens with compacted strands have a longer fatigue life. The major difference is the number of broken core wires: 42, 31, and 27 internal broken wires were found after the 35×7 rope test, respectively, set to D/d ratio of 12, 16, and 20. Considering that the number of wires constituting the core is 133, it has again been demonstrated that most broken wires occur internally in rotation-resistant ropes. Therefore, the strand's compaction reduces the number of internal breaks, resulting in core damage control (the 35×K7 tests had a small number of core breaks).

The main values of the two tests are shown in Table 7.

Table 7. The number of cycles when the discard criteria and stop criteria are reached for 35×7 rope tests, with the comparison of internal breaks for compacted ($\bar{B}_{\text{int-k}}$) and non-compacted ropes ($\bar{B}_{\text{int-nk}}$)

D/d ratio	$\bar{N}_{\text{disc}}$	$\bar{N}_{\text{stop}}$	$\bar{B}_{\text{int-k}}$	$\bar{B}_{\text{int-nk}}$
12	14920	21980	9	42
16	21980	30100	9	31
20	63500	83800	26	27

3.6 Re-lubrication effect

Re-lubrication during service is a common practice to reduce the friction between the rope elements and improve steel wire rope fatigue resistance. Two tests were carried out with the following parameters: 8×K26WS-EPIWRC specimen, D/d=12, and speed rotation set to 105 RPM; in a test, the specimen was lubricated at N=3000 and N=6000 using castor oil applied by manual brushing, while the other test was carried out on un-lubricated specimen. The results are shown in Fig.10, where it can be seen that re-lubrication delays the wire breaking.

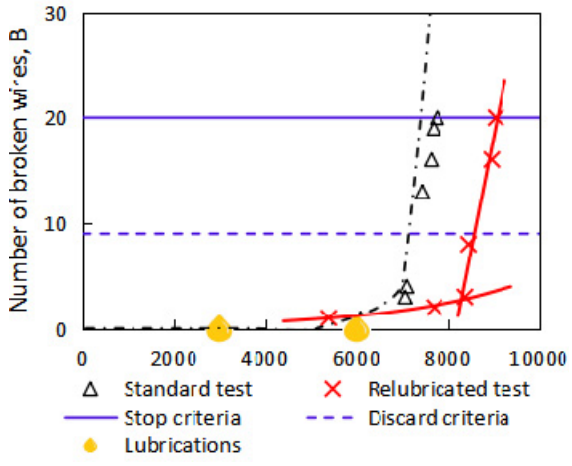

Figure 10. The trend of the first three points (red line) indicates the effect of the re-lubrication on the rope life; the lubrication was carried out at N=3000 and N=6000.

The breaking rate after the first wire break is, in fact, lower for the re-lubricated specimen, but this effect vanishes after about 2000 cycles, after which the breaking rate becomes again almost equal for the two tests. It is possible to state that the re-lubrication of a rope does not imply a significant increase in fatigue life if it is not periodically replicated.

4. DISCUSSION

4.1 Broken wires' distribution law

According to the performed tests, the number of broken wires can be related to the bending fatigue life of the specimen by the equation:

$$B = a_0 \cdot e^{a_1 N} \tag{1}$$

where B is the number of broken wires, a_0 and a_1 are the coefficients that describe the exponential function for each test, and N is the number of bending cycles.

Table 8 are listed all the tests carried out during this study.

As it can be noted, the coefficient of determination R^2 presents a high value for all the tests; it is, in particular, always higher than 0.90, with the exception of two tests on the 6×K31 rope specimens, for which it resulted in 0.82. This is probably due to a different rope construction quality along its length, especially regarding the compaction.

4.2 Predictive analysis

One of the aims of this study is to provide an instrument that can help define an optimum frequency of the periodic inspections on the rope. This definition is based on the experience of the individual inspectors or on the history of previous ropes installed on the same equip–ment, therefore without any generally accepted and verified method.

According to [33], the wire breaks distribution evokes the so-called Bathtub curve used to describe the failure rate of industrial plants and to schedule their maintenance; the M.A.P.E. indicator (Mean Absolute Percentage Error) is then used to assess the reliability of the prediction of rope failures in the cableway studied system. The Bathtub curve seeks to describe the varia–tion of the failure rate of components during their life: in our case, the component is the single wire, and the failure rate is described by the exponential trends found experimentally.

An attempt is here made to propose a similar app–roach to [33]: the procedure is based on the observation of the first two-wire breaks, then determining the exponential function passing for these points (plus the origin), thus predicting the number of cycles $\bar{N}_{\text{disc}}$ leading to the discarding condition and the number of cycles $\bar{N}_{\text{stop}}$ leading the stopping condition.

It was decided to use for this aim only the first two measurements because it simulates a real situation when the operator has to schedule subsequent inspections based on the first wire breaks observations: using more measurements, the prediction would obviously improve, but it would also be less useful for a maintenance procedure definition.

To check this procedure, it was applied to the results of the present test, and its effectiveness in predicting the actual rope failure was quantified by calculating the M.A.P.E.:

$$MAPE = \frac{1}{n}\sum_{i=1}^{1}\frac{A_i - P_i}{A_i} \quad (2)$$

where A_i is the actual number of cycles in which a wire break occurred during the tests, P_i is the number of cycles for a wire break predicted by the exponential function obtained from the first two measurements, *and* n is the total number of measurements.

The MAPE was calculated both up to the discarding ($MAPE_{disc}$) and the stopping limit ($MAPE_{stop}$)

In Fig.11, a comparison of actual and predicted fai–lure rates is shown as an example for the 6×K31WS-IWRC rope tests at different D/d ratios, while the MAPE indicators for each considered test are shown in Table 8.

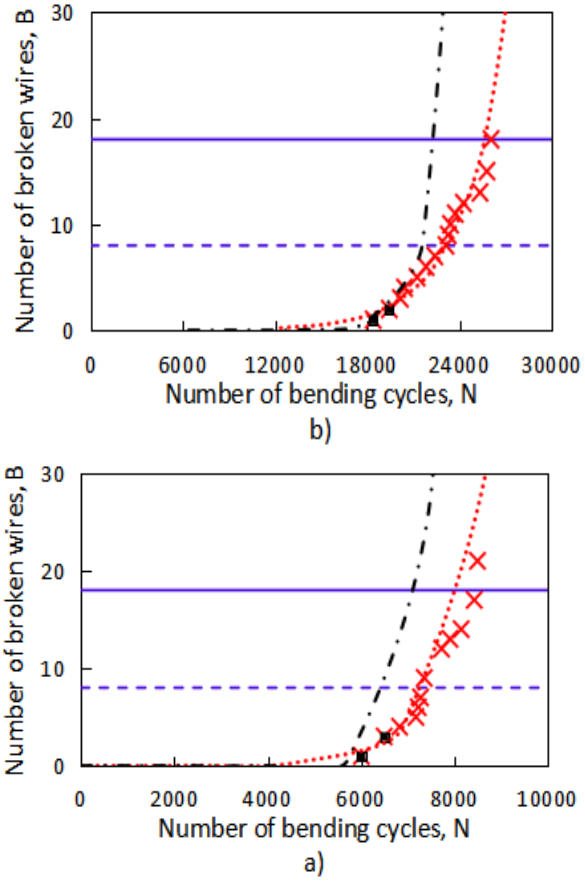

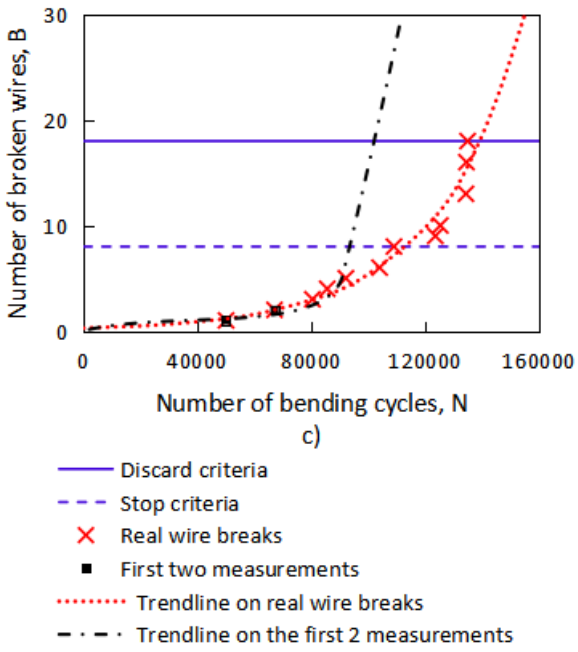

Figure 11. Tests were performed on 6×K31WS-IWRC rope at D/d=12 (a), D/d=16 (b), D/d=20 (c) at 380 RPM. The black line represents the trend that the competent person can plot using only the first two measurement points. MAPE indicates how far the two prevision

The value of the $MAPE_{disc}$[%] indicators is less than 5% in 76% of cases and a maximum value of 12.20: the predictions can be therefore considered sufficiently accurate. $MAPE_{disc}$[%]indicates the accuracy of the prediction of when to replace the rope.

4.3 Rope comparison

In order to study how the life of a rope varies with the D/d ratio, it is appropriate to transform the data acquired from absolute terms into relative terms, using a single common data. Given the importance of the discard criteria, to which a rope structure corresponds, it has been decided to compare the number of cycles at which the discard criteria is reached for each different D/d ratio (N_{disc}) to the reference one of the longest test, that is the one with D/d=20 (N_{disc20}): thus means finding the relative life, as reported in Table 9 and in Fig. 12 (examples of this approach in [19,41-43]).

Table 8. Coefficients of the exponential approximation a_0, a_1, and R^2 for each test carried out and MAPE indicators

Rope construction	d	D/d	RPM	a_0	a_1	R^2	$MAPE_{disc}$[%]	$MAPE_{stop}$[%]
8×K26WS-EPIWRC	22	12	380	0.00044	0.00110	0.97	9.02	12.52
			380	0.00095	0.00110	0.93	4.86	3.69
		16	380	0.00028	0.00055	0.92	1.03	3.27
		20	380	0.00307	0.00014	0.94	12.20	21.13
6×K31WS-IWRC	22	12	380	0.00199	0.00110	0.95	2.84	5.57
		16	380	0.00346	0.00033	0.94	6.74	9.86
		20	380	0.26260	0.00003	0.98	2.94	6.80
35×K7	24	12	380	0.00001	0.00083	0.96	0.30	3.28
		16	380	0.00039	0.00023	0.94	2.27	6.41
		20	380	0.01253	0.0006	0.98	2.66	5.98
35×7	24	12	380	0.000002	0.00096	0.93	1.26	5.28
		16	380	0.06481	0.00017	0.91	2.17	5.00
		20	380	0.16528	0.00005	0.95	7.40	18.30
8×25F-EPIWRC	22	16	220	0.06005	0.00045	0.98	3.89	11.69
	24	16	220	0.00962	0.00022	0.97	2.61	7.50

Table 8. Life behaviors related to D/d=20 tests

	8×K26WS-EPIWRC		6×K31WS-IWRC		35×K7	
D/d	N_{disc}	$\frac{N_{disc1}}{N_{disc20}}$	N_{disc1}	$\frac{N_{disc1}}{N_{disc20}}$	N_{disc1}	$\frac{N_{disc1}}{N_{disc20}}$
12	8300	0.14	7360	0.07	14550	0.15
16	18310	0.30	23140	0.21	39430	0.41
20	60490	1	108950	1	95480	1

From these exponential curves, it can be seen that the D/d variation has less consequences for the rotation-resistant rope 35×K7 than the 6×K31: for the first rope, changes from a D/d = 20 to a D/d = 12 reduces its life to 15%, while for the second rope to 7%. It can therefore be deduced that stranded ropes are more susceptible to the reduction of D/d than rotation-resistant ropes.

As regards broken wires, the damage of a rope can be described as 100% when the broken wires have reac–hed the number required by the discard criteria ($\bar{B}_{disc}$).

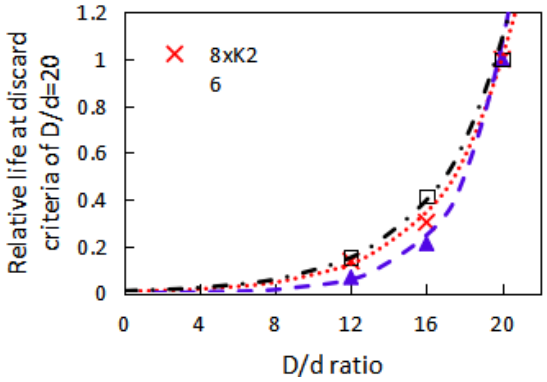

Figure 11. Relative life for different ropes subjected to different D/d ratio

It follows that the relative rope damage is defined as the ratio between the number of broken wires $\bar{B}_i$ (where i is thei-th broken wire calculated from the trend line equation of each test) and the number of broken wires of the discard:

$$D_{\%} = \frac{\bar{B}_i}{\bar{B}_{disc}} \tag{3}$$

For example, when the first wire of a 8×K26WS-EPIWRC test breaks (for this rope, the discard criteria is set to 9 broken wires), the damage is equal to one-ninth (approx.11%).

Therefore, it is possible to relate the relative rope damage with the relative life, thus finding when the breaks occur in relation to the discard criteria for each rope (Fig. 13 a,b,c).

With regard to the 8×K26, the progression of the damage is almost constant with the D/d ratio. This leads to a valuable consideration: for example, the 10% of the visible damage corresponds to 70% of its life, in particular independently from the load (D/d curves are overlapped); this means that if during an inspection, a 10% damage is found (i.e., one broken wire due to fatigue), the rope has reached 70% of its life, and consequently it has 30% of life available.

This characteristic found in eight-strand ropes is of particular importance since it allows us to state that the evolution of the rope damage by varying the stress value is stable with respect to the fatigue life. It is probably due to the geometry of the rope structure (contact angles between the strands, external profile, compaction level, etc.), which makes it more performing from this point of view.

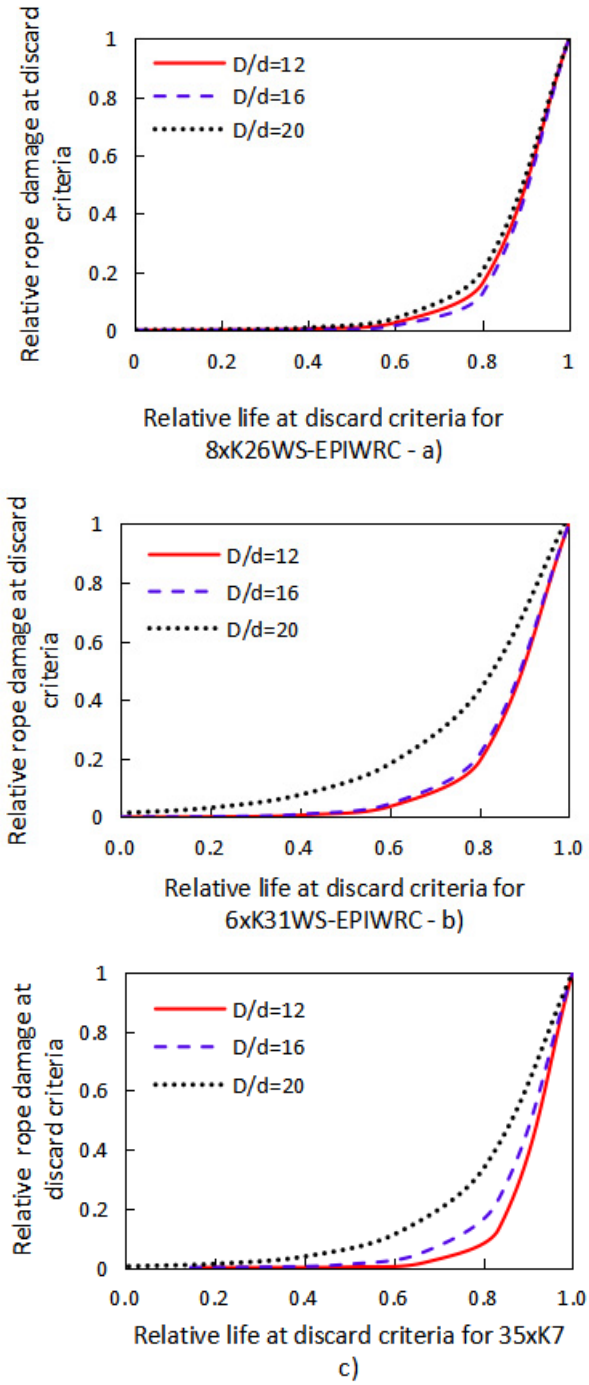

Figure 12. How the rope damage evolves with respect to the rope life

The 6×K31 rope has a similar behavior for D/d ratios set to 12 and 16, while for D/d=20, the rope damage begins to occur earlier, but it has developed slowly relative to the discard criteria. This could be an advantage because it means that the rope warns the inspector before reaching its life end; at the same time, it indicates that the rope does not work properly because some wires break too early compared to others (it is probably partly due to production problems). It can also

be seen that the rope damage evolves differently as the stress level, but it always remains exponential.

The trends of the 35×K7 are closer to each other but are separated by 20 percentage points in correspondence with the 10% damage. It should also be remembered that its discard criteria are set at three broken wires, so a single break already indicates damage of 33%, corres–ponding to the relative life of 90%.

These graphs relate the rope damage reached at a specified number of cycles, in non-dimensional terms and therefore extendable to any field of rope applica–tions: whether the rope during its life completes 10,000 or 100,000 cycles of bending over sheaves, for this method is irrelevant because it is explicit in percentage terms. It also gives us important information regarding the speed of propagation of the rope damage by looking at the curve, telling us how the speed of the damage (i.e., wire breaks) increases exponentially in the last part of its remaining life, hence the need to intervene before the curve increases its slope perilously.

It is interesting to analyze how different the trends of the studied ropes at the same D/d ratio (Fig.14a,b,c) extended until the stop criteria in order to observe the phenomenon beyond the limits suggested by the ISO 4309 Standard.

The trend lines of the ropes studied are the same as those in Fig.13, and the individual wire breaks are highlighted. As can be seen, the trends are the same for all the types of ropes: it means that the evolution of fatigue rope damage is independent of the rope const–ruction and qualitatively equal to the load. For example, it can be seen that for the rotation-resistant ropes (35×7), the first wire breaks on average at about 85% of the relative life, with rope damage corresponding to 33%.
These graphs in which the individual wire breaks are highlighted allow us to make further considerations. By the example of the 8×K26 rope trend in Fig. 14c, it can be seen that the curve is not defined before a relative life equal to about 70% (the moment when the first wire breaks): this means that if the rope is inspected at a time of life between 0 and 0.7, it will not be possible to know the percentage of life passed (and consequently the remaining one) because the rope damage is not measurable as there are no broken wires. When the first wire appears, it will be possible to draw the function, and with the second break, the drawn curve will be as reliable as described in the previous point 3.2. Instead, as previously written, the 6×K31-IWRC rope is more "safe" since the first wires broke at 40% of their life, and it was possible to draw the curve earlier.

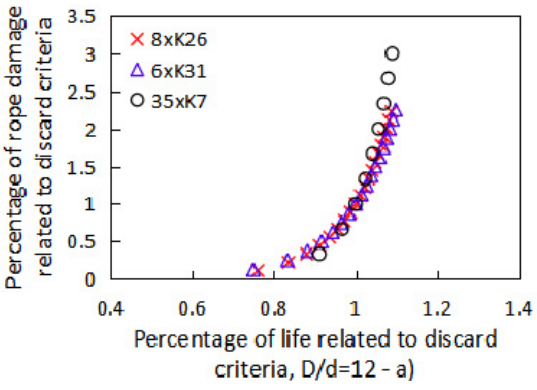

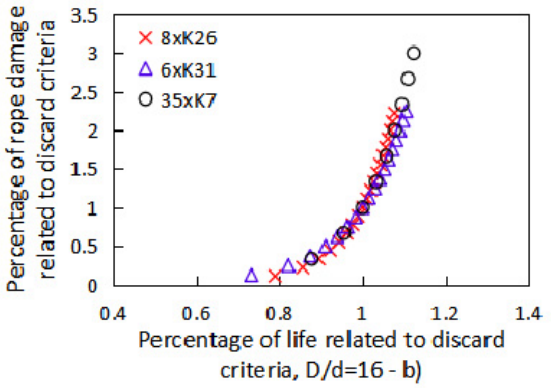

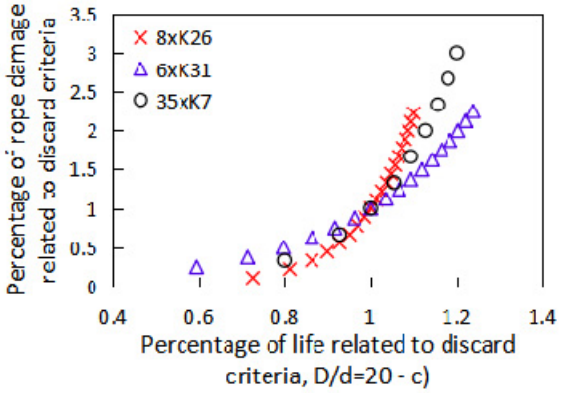

Figure14. Comparison between different ropes categories for different D/d ratios

5. CONCLUSION

An experimental methodology was proposed to analyze and quantify the evolution of fatigue damage in steel wire ropes subjected to cyclic bending. A rotary bending fatigue machine is used for this aim, composed of two counter-rotating spindles, excluding the nume–rous variables which enter in a bending over sheave test; the damage progression is monitored and defined in terms of broken wires as a function of cycling loading in the rope. This approach allows the study of the rope behavior in a simple, controlled, and repeatable way; it results efficiently in terms of time and quality of the results, applying an easy and effective standard test methodology useful for rope characterization and comparison.

The testing methodology has been applied and vali–dated on two families of wire ropes: stranded ropes (eight and six strands) and rotation-resistant ropes. Two rope endurance limits, in terms of applied loading cycles, were defined: a "discarding limit $\bar{N}_{disc}$", corresponding to the number of the visible wire breaks defined by ISO 4309:2017, and a "stopping limit $\bar{N}_{stop}$", corresponding to the number of external broken wires equal to a quarter of the total for stranded ropes, and three times the number of the corresponding discarding limit for rotation resistant ropes.

Numerous tests were carried out on rope samples (Table 1) by varying the bending stress level (D/d = 12,16,20)and the rope rotating speed (220-380 RPM) (i.e., the cycling load frequency). Some additional tests were conducted to study the effects of rope diameter, compaction, and re-lubrication. All the test results

showed that the progressive wire breaks increase with the number of bending cycles following an exponential law, independently from the construction of the rope and the bending stress level. The data obtained have been reported and analyzed in normalized form by rela–ting each rope the relative damage with the relative life at the discard in order to generalize them and to allow ensure an easier and correct reading of them, together with a proper comparison of different ropes' behaviors.

Based on experimental results, an attempt was then carried out to predict the rope endurance starting from observing the first two-wire breaks. This approach is always conservative, thus allowing a proper evaluation for subsequent rope inspections or replacement: it appe–ars, therefore, suitable for predicting the broken wires' progression in those applications where the rope is mainly discarded due to fatigue, and it can be used both to assess ropes during their use on new installations and to assess the residual fatigue life in post-retirement analyses.

ACKNOWLEDGMENTS

The authors would like to acknowledge the engineer Franco Clerici of the Usha Martin Company for his support in the experimental tests.

REFERENCES

[1] Hall HM.: Stresses in small wire ropes. Wire Wire Prod 1951;26:257–9.

[2] F.H. H.: Tangential forces in wire ropes. Wire Wire Prod 1953;28:455–60.

[3] Leissa AW.: Contact stresses in wire ropes. Wire Wire Prod 1959;34:307–14, 372–3.

[4] Starkey WL, Cress HA.: An analysis of critical stresses and mode of failure of a wire rope. J EngInd Trans ASME 1959;81:307–16.

[5] Bert CW, Stein RA.: Stress analysis of wire rope in tension and torsion. Wire Wire Prod 1962;37:621–4, 769–70, 772–816.

[6] Torkar M, Arzenšek B.: Failure of crane wire rope. Eng Fail Anal 2002;9:227–33. Peterka P, KrešákJ, Kropuch S, Fedorko G, Molnar V, Vojtko M. Failure analysis of hoisting steel wire rope. Engineering Failure Analysis 2014;45:96–105.

[7] Peterka P, Krešák J, Kropuch S, Fedorko G, Molnar V, Vojtko M.: Failure analysis of hoisting steel wire rope. Engineering Failure Analysis2014;45:96–105.

[8] Palit P, Kushwaha SK, Mathur J, Chaturvadi AK.: Life Cycle Assessment of Wire Rope Used in Crane Application in a Steel Plant. Journal of failure analysis and prevention 2019;19:752–60.

[9] Bennetts I, Moinuddin K.: Evaluation of the impact of potential fire scenarios on structural elements of a cable-stayed bridge. Journal of Fire Protection Engineering 2009;19:85–106.

[10] Rosakis P., et al.: Partition of plastic work into heat and stored energy in metals. 2: Theory. ExpMech 1998:113–23.

[11] Rittel D, Zhang LH, Osovski S. The dependence of the Taylor–Quinney coefficient on the dynamic loading mode. Journal of the Mechanics and Physics of Solids 2017;107:96–114.

[12] Kastratović G, Vidanović N.: Some aspects of 3D finite element modeling of independent wire rope core. FME Transactions 2011;39-1:37-40

[13] Kastratović G, Vidanović N, Bakić V, Rašuo B.: On finite element analysis of sling wire rope subjected to axial loading. Ocean Engineering 2014;88:480–487

[14] Jiang W-G.: A concise finite element model for pure bending analysis of simple wire strand. International Journal of Mechanical Sciences 2012;54:69–73.

[15] Cruzado A, Leen SB, Urchegui MA, Gómez X.: Finite element simulation of fretting wear and fatigue in thin steel wires.International Journal of Fatigue 2013;55:7–21.

[16] Cruzado A, Urchegui MA, Gómez X.: Finite element modeling of fretting wear scars in the thin steel wires: Application in crossed cylinder arrangements. Wear 2014;318:98–105.

[17] Wang D, Zhang D, Ge S.: Finite element analysis of fretting fatigue behavior of steel wires and crack initiation characteristics. Engineering Failure Analysis2013;28:47–62.

[18] Wang D, Zhang D, Wang S, Ge S.: Finite element analysis of hoisting rope and fretting wear evolution and fatigue life estimation of steel wires. Engineering Failure Analysis2013;27:173–93.

[19] Mouradi H, El Barkany A, El Biyaali A.: Steel Wire Ropes Failure Analysis: Experimental Study. Engineering Failure Analysis 2018; 91:234–42.

[20] Utting WS, Jones N.: The response of wire rope strands to axial tensile loads—Part II. Comparison of experimental results and theoretical predictions. International Journal of Mechanical Sciences 1987; 29:621–36.

[21] Utting WS, Jones N.: The response of wire rope strands to axial tensile loads—Part I. Experimental results and theoretical predictions. International Journal of Mechanical Sciences 1987;29:605–19.

[22] Wahid A. et al.: Energy method for experimental life prediction of central core strand constituting a steel wire rope. Engineering Failure Analysis 2019; 97:61–71.

[23] Wahid A, Mouhib N, Ouardi A, Sabah F, Chakir H, ELghorba M.: Experimental prediction of wire rope damage by energy method. Engineering Structures 2019;201:109794.

[24] Wang D, Zhang D, Ge S.: Fretting-fatigue behavior of steel wires in low cycle fatigue. Mater Des 2011;32:4986–93.

[25] Battini D, Solazzi L, Lezzi AM, Clerici F, Donzella G.: Prediction of steel wire rope fatigue life based on thermal measurements. International Journal of Mechanical Sciences 2020;182:105761.

[26] Curà F, Curti G, Sesana R.: A new iteration method for the thermographic determination of fatigue limit in steels. Int J Fatigue 2005;27:453–9.

[27] Wang XG, Crupi V, Guo XL, Guglielmino E.: A thermography-based approach for structural analysis and fatigue evaluation. Proc Inst MechEng Part C Journal of Mechanical Engineering Science 2012;226:1173–85.

[28] Pal U, Mukhopadhyay G, Sharma A. Bhattacharya S.: Failure analysis of wire rope of ladle crane in steel making shop. International Journal of Fatigue, 2018;116:149-55.

[29] Singh R.P, Mousumi Mallick M, &, M.K. Verma.: Studies on failure behaviour of wire rope used in underground coal mines. Engineering Failure Analysis, 2016;70:290–304.

[30] Wokem C, Joseph TG, Curley M.: Fatigue prediction for hoist cables over sheaves in large mining shovel application. Fatigue & Fracture of Engineering Materials & Structures 2018;41:1838–52.

[31] Abdulhamid MF, Kamarudin M, Kang HS, Kader AS, Tamin MN, Ahmad S, et al.: Numerical Framework for Fatigue Life Prediction of Steel Wire Ropes Employing Damage-based Failure Models. Proceedings of the 29th European Safety and Reliability Conference (ESREL), Research Publishing Services; 2019; 2135–41.

[32] Zhao D, Gao C, Zhou Z, Liu S, Chen B, Gao J.: Fatigue life prediction of the wire rope based on grey theory under small sample condition. Engineering Failure Analysis 2020;107:104237.

[33] Peterka P, Kačmáry P, Krešák J, Šimoňák J, Bindzár P, Mitrík D.: Prediction of fatigue fractures diffusion on the cableway haul rope. Engineering Failure Analysis 2016;59:185–96.

[34] Zhang D, Feng C, Chen K, Wangb D, Ni X.: Effect of broken wire on bending fatigue characteristics of wire ropes. International Journal of Fatigue, 2017;103:456–65.

[35] Zhang D, Chen K, Jia X, Wangb D, Wangb S, Luo Y, Ge S.: Bending fatigue behaviour of bearing ropes working around pulleys of different materials. Engineering Failure Analysis, 2013;33: 37–47.

[36] Feyrer K.: Wire ropes: tension, endurance, reliability. Springer Berlin Heidelberg, 2015.

[37] Thompson E, Basua R, Loosb T.: Wire failure prediction for a rotary beam fatigue tester. Case Studies in Non destructive Testing and Evaluation, 2014; 2:1–8.

[38] Onur Y. A., İmrak C.E.: The influence of rotation speed on the bending fatigue lifetime of steel wire ropes. Proceedings of the Institution of Mechanical Engineers, Part C: Journal of Mechanical Engineering Science, Mar. 2011;225-3:520–25.

[39] Zhao D, Liu S, Xu Q, Shi F, Sun W, Chai L.: Fatigue life prediction of wire rope based on stress field intensity method. Engineering Failure Analysis, 2017; 81:1–9.

[40] Giglio M, Manes A. Life prediction of a wire rope subjected to axial and bending loads. Engineering Failure Analysis, 2005;12-4:549–68.

[41] Ye H, Duan Z, Tang S, Yang Z, Xu X.: Fatigue crack growth and interaction of bridge wire with multiple surface cracks. Engineering Failure Analysis, 2020;116:104739.

[42] Jikala A, Majidb F, Chaffouia H, Mezianec M, ELghorbab M.: Corrosion influence on lifetime prediction to determine the Wöhler curves of outer layer strand of a steel wire rope. Engineering Failure Analysis, 2020; 109:104253.

[43] Mouhib N, Achraf Wahid A, Sabah F, Chakir H, ELghorba M.: Experimental characterization and damage reliability analysis of central core strand extracted from steel wire rope. Engineering Failure Analysis, 2021;120:105103.

NOMENCLATURE

d	Rope diameter
D	Distance between spindle centers
B	Number of broken wire
$\bar{B}_i$	i-th broken wire
$\bar{B}_{disc}$	Number of broken wires, according to the discarding criterion
$\bar{B}_{stop}$	Number of broken wires for which the test is stopped
$\bar{B}_{\text{int-k}}$	Number of internal broken wires for compacted rope tests
$\bar{B}_{\text{int-nk}}$	Number of internal broken wires for non-compacted rope tests
$MAPE_{disc}$	MAPE calculated at discard criteria
$MAPE_{stop}$	MAPE calculeted at stop limit
N	Number of bending cycles
$\bar{N}_{disc}$	Number of bending cycles when the discarding limit is reached
$\bar{N}_{stop}$	Number of bending cycles when the stopping limit is reached
R^2	Coefficient of determination
T	Temperature
ΔT	Temperature variation with respect to room temperature

Acronyms

IWRC	Independent wire rope core
EPIWRC	Independent plastic-coated rope core
WS	Warrington-seal rope
K	Compacted rope
RH	Right-hand rope
LH	Left-hand rope
OL	Ordinary-lay rope
LL	Lang-lay rope
RPM	Revolutions per minute
MAPE	Mean Absolute percentage error

ПРЕДВИЂАЊЕ ЗАМОРНОГ ВЕКА САВИЈАЊА УЖЕТА НА ОСНОВУ БРЗИНЕ ЛОМЉЕЊА ЖИЦЕ

П. Фреди, Л. Солаци, Г. Донзела

Челична жичана ужад нуде безбедносне перфор–мансе независне од произвођача, док перформансе издржљивости могу бити различите. За процену статуса оштећења жичаног ужета у току његовог сервисирања користе се методе безбедне од квара,

па је за њихову примену неопходно знати прогресију оштећења. Овај рад предлаже аналитичку методу за процену заморног века челичних ужади. Користећи бездимензионалну анализу, предложена је карактеристична крива оштећења за сваку категорију ужади, постављајући основу за предиктивну процедуру одржавања која се може проширити на све области примене ужади где је замор при савијању први критеријум одбацивања за замену ужета. Испитивања замора при ротационом савијању се изводе на различитим узорцима конструкције ужади и прати се еволуција прекинутих жица. Показало се да је тренд нивоа лома експоненцијалан са временом, без обзира на врсту ужета и ниво напрезања.